

CAN EXTRAGALACTIC FOREGROUNDS EXPLAIN THE LARGE-ANGLE CMB ANOMALIES?

Aleksandar Rakić¹, Syksy Räsänen² and Dominik J. Schwarz¹

¹ *Fakultät für Physik, Universität Bielefeld, Postfach 100131, D-33501 Bielefeld Germany*

² *CERN Physics Department Theory Unit, CH-1211 Geneva 23, Switzerland*

email: rakic at physik dot uni-bielefeld dot de, syksy dot rasanen at iki dot fi,

dschwarz at physik dot uni-bielefeld dot de

We address the effect of an extended local foreground on the low- ℓ anomalies found in the CMB. Recent X-ray catalogues point us to the existence of very massive superstructures at the $100 h^{-1}\text{Mpc}$ scale that contribute significantly to the dipole velocity profile. Being highly non-linear, these structures provide us a natural candidate to leave an imprint on the CMB sky via a local Rees-Sciama effect. We show that the Rees-Sciama effect of local foregrounds can induce CMB anisotropy of $\Delta T/T \sim 10^{-5}$ and we analyse its impact on multipole power as well as the induced phase pattern on largest angular scales.

1. Motivation and Overview

At largest angular scales which correspond to small multipole moments ℓ there exist puzzling features in the Cosmic Microwave Background (CMB). The near vanishing of the two-point angular correlation function in all wavebands for angular scales between 60° and 170° is one of the longest known anomalies, already detected in the data of the Cosmic Background Explorer's Differential Radiometer (COBE-DMR). It has been confirmed and persists in the three-year Wilkinson Microwave Anisotropy Probe data [WMAP(3yr)].^{1,2} Among the two-point angular correlation functions it has been shown that none of the almost vanishing cut-sky wavebands matches the full sky and again neither one of these is in accordance with the best fit Λ cold dark matter (ΛCDM) model.³ The disagreement turned out to be even more distinctive in the WMAP(3yr) data than in WMAP(1yr) and is unexpected at 99.97% C.L. for the updated Internal Linear Combination map [ILC(3yr)].³

Besides the lack of power, there are a number of remarkable anomalies regarding the phase relationships of the quadrupole and octopole within the WMAP data.⁴⁻⁶ In order to be able to make distinct statements with respect to a phase analysis of multipoles we make use of the *multipole vectors formalism*.⁷ Looking at quadrupole plus octopole vectors from WMAP(3yr) the alignment with the equinox (EQX) and with the ecliptic is found to be unlikely at 99.8% C.L. and 96% C.L. respectively.³ The correlation with the dipole direction and with the galactic plane is found to be odd at 99.7% C.L. and 99% C.L. respectively. Moreover from the combined full sky map of $\ell = 2 + 3$ one infers that the octopole is quite planar and that the ecliptic strongly follows a zero line of the map, leaving the two strongest extrema in the southern hemisphere and the two weakest in the northern hemisphere. Some of these effects are statistically dependent, e.g. given the observed quadrupole-octopole alignment, the significance of alignment with the galactic plane is reduced to unremarkable 88% C.L.

These findings support the conclusion that either the Universe as seen by WMAP

is not statistically isotropic on largest scales, or that the observed features are due to unexpected foregrounds, hidden systematics or new physics challenging the standard cosmological model. Diverse attempts for explanation can be found in the literature: considering anisotropic or inhomogeneous models [Bianchi family, Lemaître–Tolman–Bondi (LTB) models],^{8–13} Solar system foreground,¹⁴ lensing of the CMB¹⁵ and moving foregrounds,¹⁶ Sunyaev–Zel’dovich (SZ) effect^{17,18} and Rees-Sciama (RS) effect,^{12,19} considering a non-trivial topology of the Universe,^{20,21} considering modifications and refinements of the standard simplest scenario of inflation,^{22–28} considering possible phenomenology of loop quantum gravity.^{29,30} In this talk we update and expand our previous work¹² in the light of the WMAP(3yr) data release.

2. Local Structures and Rees-Sciama Effect

Recent X-ray catalogues of our neighborhood show that a major contribution to the dipole velocity profile originates from the Shapley Supercluster (SSC) and other density concentrations at a distance of around $130\text{--}180 h^{-1}$ Mpc.^{31–34} The SSC is a massive concentration centered around the object A3558 with a density contrast of $\delta \simeq 5$ over the inner $30 h^{-1}$ Mpc region.³⁵

We will show that the CMB displays correlations between the dipole and higher multipoles after passing through non-linear structures, due to the RS effect.³⁶ The physics of the RS effect is that in the non-linear regime of structure formation, the gravitational potential changes with time, so photons climb out of a slightly different potential well than the one they fell into. Following ref.³⁷ the CMB anisotropy produced by a spherical superstructure is estimated by the integral of the gravitational potential perturbation $\phi \simeq \delta M/d$ along the path of the photon: $\Delta T(\theta, \varphi)/T \simeq \phi v_c$, where d is the physical size of the structure and δM is the mass excess. Here we assumed a structure collapsing at velocity v_c and let the evolution time of the structure t_c be the matter crossing time d/v_c (using $c \equiv 1 \equiv G$). We estimate the typical collapse velocity from the energy balance condition $v_c^2 \simeq \phi$ and get: $\Delta T(\theta, \varphi)/T \sim \phi^{3/2} \sim (\delta M/d)^{3/2}$. We model the non-linear structure by a spherically symmetric LTB model embedded in a flat ($\Omega = 1$) Friedmann–Robertson–Walker Universe. Substituting the expression for the mass excess within this model we arrive at:³⁷

$$\frac{\Delta T(\theta, \varphi)}{T} \sim \left(\frac{\delta\rho}{\rho}\right)^{3/2} \left(\frac{d}{t}\right)^3, \quad (1)$$

where t is the cosmic time at which the CMB photons crossed the structure.

Inserting the characteristics of the SSC it follows that a *CMB anisotropy of 10^{-5} due to a local RS effect is reasonable*. For simplicity we picture the local Universe as a spherically symmetric density distribution, with the Local Group (LG) falling towards the core of the overdensity at the centre. The line between our location and the centre defines a preferred direction \hat{z} , which in the present case corresponds to the direction of the dipole. This setup exhibits rotational symmetry w.r.t. the axis \hat{z} (neglecting transverse components of our motion). Consequently, only zonal

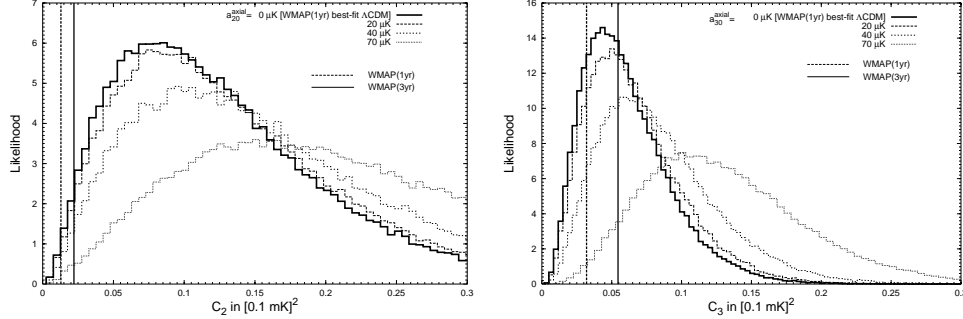


Fig. 1. Likelihood of quadrupole and octopole power for increased axial contributions. Vertical lines denote experimental data: WMAP(1yr) cut-sky and WMAP(3yr) maximum likelihood estimate. Considering the quadrupole adding *any* multipole power was excluded at $> 99\%$ C.L. w.r.t WMAP(1yr) but it is possible to add up to $60\mu\text{K}$ within the same exclusion level w.r.t. the WMAP(3yr) value. The octopole is more resistant against axial contaminations as it is possible to add a whole $100\mu\text{K}$ before reaching the same exclusion level w.r.t the updated WMAP data.

harmonics ($m = 0$ in the \hat{z} -frame) are generated. Note that any other effect with axial symmetry would also induce anisotropy only in the zonal harmonics.

3. Multipole Analysis

We study how maps of the CMB are affected by the anisotropy induced by additional axisymmetric contributions $a_{\ell 0}^{\text{axial}}$ added to the quadrupole and octopole by using Monte Carlo (MC) methods. As predicted by the simplest inflationary models, we assume that the $a_{\ell m}$ are fully characterised only by angular power, for which we use the values from the best fit ΛCDM temperature spectrum to the WMAP data.² We produced 10^5 MC realisations of $\ell = 2$ and $\ell = 3$ for the statistical analysis.

The angular power spectrum is estimated by $C_\ell = 1/(2\ell + 1) \sum_m |a_{\ell m}|^2$. In fig. 1 we show how the histograms for the quadrupole and octopole power compare with the measured values from WMAP(1yr,3yr). Considering the WMAP(1yr) cut-sky, adding *any* power to the quadrupole was already excluded at $> 99\%$ C.L. whereas the WMAP(3yr) data allows for adding up to $a_{20}^{\text{axial}} = 60\mu\text{K}$ in order to reach the same exclusion level. The octopole is quite robust against axial contaminations as it lies better on the fit: in order to reach the same exclusion level of $> 99\%$ C.L. it is necessary to add $a_{30}^{\text{axial}} = 80\mu\text{K}$ w.r.t. the WMAP(1yr) cut-sky and a whole $a_{30}^{\text{axial}} = 100\mu\text{K}$ w.r.t. the WMAP(3yr) value. Considering only the WMAP(3yr) maximum likelihood estimate and increasing the effect of local structures up to $a_{\ell 0}^{\text{axial}} = 70\mu\text{K}$ leads to an exclusion of 99.5% C.L. for C_2 and 92.9% C.L. for C_3 .

The next question is what kind of phase pattern the contribution $a_{\ell 0}^{\text{axial}}$ will induce on the CMB sky. Using the multipole vector formalism⁷ a (temperature) multipole on a sphere can be alternatively decomposed as:

$$T_\ell = \sum_{m=-\ell}^{\ell} a_{\ell m} Y_{\ell m}(\theta, \varphi) = A^{(\ell)} \left[\prod_{i=1}^{\ell} \left(\hat{\mathbf{v}}^{(\ell, i)} \cdot \hat{\mathbf{e}}(\theta, \varphi) \right) - \mathcal{L}_\ell(\theta, \varphi) \right], \quad (2)$$

where $\hat{e}(\theta, \varphi) = (\sin \theta \cos \varphi, \sin \theta \sin \varphi, \cos \theta)$ is a radial unit vector. With the decomposition (2) it is possible to obtain a unique factorisation of a multipole into a scalar part $A^{(\ell)}$ which measures its total power and ℓ unit vectors $\hat{\mathbf{v}}^{(\ell, i)}$ that contain all the directional information. The signs of the multipole vectors can be absorbed into the scalar quantity $A^{(\ell)}$, and are thus unphysical.

Introducing the $\ell(\ell - 1)/2$ oriented areas $\mathbf{n}^{(\ell, i, j)} \equiv \hat{\mathbf{v}}^{(\ell, i)} \times \hat{\mathbf{v}}^{(\ell, j)} / |\hat{\mathbf{v}}^{(\ell, i)} \times \hat{\mathbf{v}}^{(\ell, j)}|$ we are ready to define a statistic in order to probe alignment of the normals $\mathbf{n}^{(\ell, i, j)}$ with a given physical direction $\hat{\mathbf{x}}$:

$$S_{\mathbf{n}\mathbf{x}} \equiv \frac{1}{4} \sum_{\ell=2,3} \sum_{i < j} \left| \mathbf{n}^{(\ell, i, j)} \cdot \hat{\mathbf{x}} \right|. \quad (3)$$

We test for alignment with three natural directions $\hat{\mathbf{x}}$: the north ecliptic pole (NEP), EQX and the north galactic pole (NGP). The results of the correlation analysis are shown in fig. 2: in the first row the preferred direction $\hat{\mathbf{z}}$ coincides with the direction of local motion, the dipole.³⁸ Here the anomaly becomes worse when increasing the amplitude of the axial contribution. But for $\hat{\mathbf{x}} = \text{NEP}$ the exclusion becomes somewhat milder; e.g. $a_{\ell 0}^{\text{axial}} = 40 \mu\text{K}$ leads to an exclusion of 99.2% C.L. for ILC(1yr) but only 98.2% C.L. for the updated ILC map. Finding an alignment with the EQX though is strongly excluded at $> 99.2\%$ C.L. even with a vanishing axial contribution for both one- and three-year data.

In the second row of fig. 2 we let the preferred direction point to the NEP as a complementary test. Here the probability to find an ecliptic alignment becomes dramatically increased: with a $a_{\ell 0}^{\text{axial}} = 70 \mu\text{K}$ it is 17% and 10% for the ILC(3yr) and ILC(1yr) values respectively. Regarding the three-year data the probability for finding an EQX alignment increases from 1% to 3% for $a_{\ell 0}^{\text{axial}} = 70 \mu\text{K}$. The alignment with the NGP remains quite stable for both tested directions of $\hat{\mathbf{z}}$.

4. Conclusion

Recent astrophysical data cataloguing our neighborhood in the X-ray band point us to the existence of massive non-linear structures like the SSC at distances $\sim 100 h^{-1}\text{Mpc}$. Besides its significant contribution to the dipole velocity profile such a structure is able to induce anisotropies $\sim 10^{-5}$ via its RS effect. Regarding CMB modes, the spherical symmetry (LTB) which we use to approximate the local superstructure reduces to an axial symmetry along the line connecting our position and the centre of the superstructure where we locate the SSC. We produced statistically isotropic and gaussian MC maps of the CMB and computed their S -statistics (3) for alignment with generic astrophysical directions like the NEP, EQX and NGP. The additional zonal harmonics have been added with increasing strength (see ref.³⁹ for full-sky maps). When gauging the preferred axis to the direction of local motion (WMAP dipole) the consistency of the data with theory becomes even worse, albeit with less significance w.r.t. WMAP(3yr). On the other hand an orthogonally directed (Solar system) effect would be more consistent with the three-year data.

Considering extended local foregrounds Abramo et al.¹⁷ recently proposed that a cold spot in the direction of the local Supercluster could account for the cross alignments of quadrupole and octopole. The cold spot would be realised by the SZ effect of CMB photons scattering of the hot intracluster gas. On the other hand Inoue and Silk¹⁹ suggest a certain geometrical pattern of two identical voids to account for the cross alignment as well as for the octopole planarity via the RS effect. Each of the latter approaches alone is not fully satisfactory. Nevertheless a combined approach enfolding the RS effect as well as the SZ effect from extended foregrounds seems promising for the future. Moreover, since the local RS effect can contribute up to 10^{-5} to the temperature anisotropies on large angular scales, a detailed study is important for cross-correlating CMB data (including upcoming Planck data) with astrophysical observations on the local large-scale structure.

Acknowledgment

It is a pleasure to thank the organisers of the 11th Marcel Grossmann meeting for their effort and the opportunity to speak. We acknowledge the use of the Legacy Archive for Microwave Background Data Analysis (LAMBDA) provided by the NASA Office of Space Science. The work of AR is supported by the DFG grant GRK 881.

References

1. G. Hinshaw et al., astro-ph/0603451.
2. WMAP data products at <http://lambda.gsfc.nasa.gov/>
3. C. Copi, D. Huterer, D. J. Schwarz and G. Starkman, astro-ph/0605135.
4. D. J. Schwarz, G. D. Starkman, D. Huterer and C. J. Copi, *PRL* **93**, 221301 (2004).

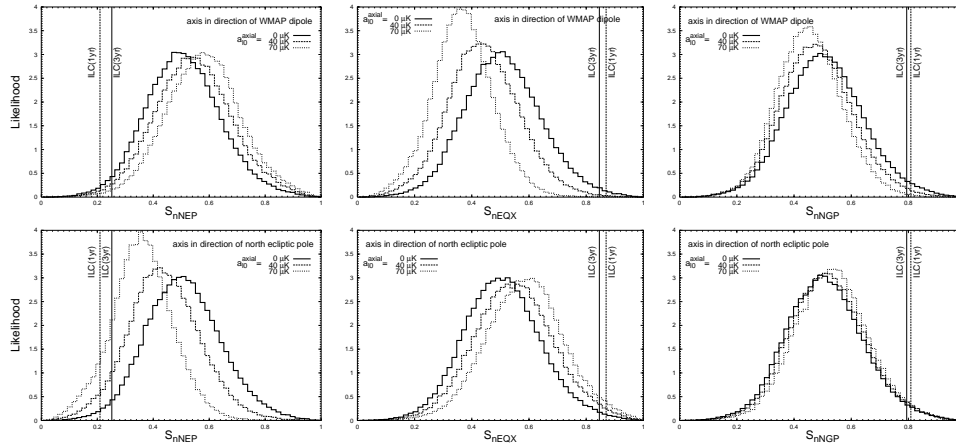


Fig. 2. WMAP one- and three-year ILC maps compared to the alignment (3) of quadrupole and octopole normals with physical directions (NEP, EQX, NGP in columns) for two orthogonal realisations of the preferred direction \hat{z} (WMAP dipole, NEP in rows). The bold histograms represent statistically isotropic and gaussian skies. Increasing the axial contribution makes the anomalies worse for $\hat{z} = \text{WMAP dipole}$, but with the exclusions being less significant for the ILC(3yr) than for the ILC(1yr). At the same time a Solar system effect is preferred by the data.

5. H. K. Eriksen, F. K. Hansen, A. J. Banday, K. M. Górski and P. B. Lilje, *ApJ* **605**, 14 (2004); (Erratum) **609**, 1198 (2004).
6. A. de Oliveira-Costa, M. Tegmark, M. Zaldarriaga and M. Hamilton, *Phys. Rev. D* **69**, 063516 (2004); A. de Oliveira-Costa and M. Tegmark, astro-ph/0603369.
7. C. J. Copi, D. Huterer and G. D. Starkman, *Phys. Rev. D* **70**, 043515 (2004).
8. T. Ghosh, A. Hajian and T. Souradeep, astro-ph/0604279.
9. T. R. Jaffe, A. J. Banday, H. K. Eriksen, K. M. Gorski and F. K. Hansen, astro-ph/0606046 and references therein.
10. H. Alnes and M. Amarzguoui, astro-ph/0607334.
11. J. W. Moffat *JCAP* **0510**, 012 (2005).
12. A. Rakić, S. Räsänen and D. J. Schwarz, *MNRAS* **369**, L27 (2006).
13. K. Tomita *Phys. Rev. D* **72**, 043526 (2005), *Phys. Rev. D* **72** 103506; (Erratum) **D 73** 029901.
14. P. C. Frisch, *ApJ* **632**, L143 (2005).
15. C. Vale, astro-ph/0509039.
16. A. Cooray and N. Seto, *JCAP* **0512**, 004 (2005).
17. L. R. Abramo and L. Sodré Jr., astro-ph/0312124;
L. R. Abramo, L. Sodré Jr. and C. A. Wuensche, astro-ph/0605269.
18. F. K. Hansen, E. Branchini, P. Mazzotta, P. Cabella and K. Dolag, *MNRAS* **361**, 753 (2005).
19. K. T. Inoue and J. Silk, *ApJ* **648**, 23 (2006); K. T. Inoue and J. Silk, astro-ph/0612347.
20. A. Riazuelo, J. Weeks, J. P. Uzan, R. Lehoucq and J. P. Luminet, *Phys. Rev. D* **69**, 103518 (2004); J. P. Luminet, J. Weeks, A. Riazuelo, R. Lehoucq and J. P. Uzan, *Nature* **425**, 593 (2003).
21. J. Shapiro Key, N. J. Cornish, D. N. Spergel and G. D. Starkman, astro-ph/0604616; N. J. Cornish, D. N. Spergel, G. D. Starkman and E. Komatsu, *Phys. Rev. Lett.* **92**, 201302 (2004).
22. D. Boyanovsky, H. J. de Vega and N. G. Sanchez, astro-ph/0607508; astro-ph/0607487.
23. L. Campanelli, P. Cea and L. Tedesco, astro-ph/0606266.
24. C. R. Contaldi, M. Peloso, L. Kofman and A. Linde, *JCAP* **0307**, 002 (2003).
25. F. Ferrer, S. Räsänen and J. Väliviita, *JCAP* **0410**, 010 (2004).
26. C. Gordon and W. Hu, *Phys. Rev. D* **70**, 083003 (2004).
27. A. E. Gümriükçüoğlu, C. R. Contaldi and M. Peloso, astro-ph/0608405.
28. C.-H. Wu, K.-W. Ng, W. Lee, D.-S. Lee and Y.-Y. Charng, astro-ph/0604292.
29. S. Hofmann and O. Winkler, gr-qc/0411124.
30. S. Tsujikawa, P. Singh and R. Maartens, *CQG* **21**, 5767 (2004).
31. D. D. Kocevski, C. R. Mullis, H. Ebeling, *ApJ* **608**, 721 (2004).
32. D. D. Kocevski, H. Ebeling, *ApJ* **645**, 1043 (2006).
33. M. J. Hudson, R. J. Smith, J. R. Lucey, E. Branchini, *MNRAS* **352**, 61 (2004).
34. J. Lucey, D. Radburn-Smith, M. Hudson, astro-ph/0412329.
35. D. Proust et al., *A&A* **447**, 133 (2006).
36. M. J. Rees, D. W. Sciama, *Nature* **217**, 511 (1968).
37. M. Panek, *ApJ* **388**, 225 (1992).
38. C. L. Bennett et al., *ApJS* **148**, 1 (2003).
39. Full-sky maps at <http://www.physik.uni-bielefeld.de/cosmology/rs.html>